

Investigation of epoxy resin/multiwalled carbon nanotube nanocomposite behavior at low frequency

Mauro Giorcelli^{a)}

Department of Applied Science and Technology, Politecnico di Torino, Corso Duca degli Abruzzi 24, Torino 10129, Italy

Patrizia Savi, Muhammad Yasir, Mario Miscuglio, and Muna Hajj Yahya

Department of Electronic and Telecommunication, Politecnico di Torino, Corso Duca degli Abruzzi 24, Torino 10129, Italy

Alberto Tagliaferro

Department of Applied Science and Technology, Politecnico di Torino, Corso Duca degli Abruzzi 24, Torino 10129, Italy

(Received 7 July 2014; accepted 14 October 2014)

In this work, the electrical characterization of nanocomposites made of epoxy resins with multiwalled carbon nanotubes is presented. As the filler, two different types of multiwalled carbon nanotubes with different aspect ratios (280, 1250) and defectiveness were selected. The production procedure, the morphological characterization, the I - V DC characteristics, and the low frequency complex permittivity (in the range 100 kHz–12 MHz) of these nanocomposites are discussed. To investigate the dispersion of the solution, a study which linked the mixing time to the zeta potential was performed. The experimental results show that with the same matrix and by using the same measurement techniques, the two nanocomposites give different results and can be correlated with the characteristics of nanotubes. The dc conductivity of the nanocomposites was measured by means of a two-point probe technique. The conductivity in the frequency range 100 KHz–12 MHz was evaluated using a circular disk capacitor and measuring the impedance. The measured conductivity follows a percolation scaling law of the form $\sigma \propto (p - p_c)^t$. A best fit to the measured conductivity data was obtained and the values of the exponent t compared to those in the literature.

I. INTRODUCTION

Recent years have seen a significant research increase in development activities on nanocomposites (NCs) for engineering applications. Polymer NCs, especially those containing carbon nanotubes (CNTs), have proved to be particularly attractive, as the addition of CNTs leads to electrically conductive composites with enhanced structural characteristics.

Multiwalled CNTs (MWCNTs) are the most commonly used for large-scale applications because of their affordable cost (see e.g., Ref. 1 and 2). Their extraordinary properties are easily transferred to the host polymer thus improving the properties of the NC. For example, MWCNTs are frequently used as a reinforcement for polymers,^{3,4} since CNTs are much stronger and have a much larger aspect ratio (i.e., the ratio between length and diameter) than conventional carbon fibers. Alternatively, CNTs have been embedded into polymers or other media to obtain materials with good electrical and thermal properties.^{5,6}

The main advantage of MWCNTs is that only a few weight percentage (wt%) of them can greatly improve the properties of the hosting material from the mechanical and electrical point of view.⁶ The fall in production costs and the consequent increase of their availability have also made MWCNTs interesting filler materials for large-scale applications.⁷

In an insulating matrix, conductive filler particles such as MWCNTs are able to lower the overall resistivity by several orders of magnitude when their network develops throughout the matrix. The transition from an insulating to conducting behavior as a function of filler concentration is known as percolation, and the critical concentration at which this transition occurs is called the percolation threshold.^{8–11}

Conductivity, one of the most interesting and investigated properties of NCs^{12–15} from an electrical point of view, is also one of the focuses in the present work.

In this paper, two main aspects are addressed. The first one is the dispersion of CNTs in the NC, a key issue if uniform and reproducible samples fully exploiting the characteristics of MWCNTs are to be obtained. The second one is the characterization of the NCs from an electrical point of view. To this end, I - V

^{a)}Address all correspondence to this author.

e-mail: mauro.giorcelli@polito.it

DOI: 10.1557/jmr.2014.348

characteristics in DC and capacitive measurements (in the range 100 kHz–12 MHz) of the permittivity were carried out. The results are discussed in the light of filler percentage and of the characteristics of the MWCNTs. The correlation between these results and the geometrical parameters of MWCNTs will be discussed and elucidated.

II. MATERIALS AND METHODS

A. Material used

To produce the NCs, we used two different types of MWCNTs provided by Nanothinx (Greece) and grown using a catalytic chemical vapor deposition (CCVD) technique. Their geometrical characteristics (nominal length, diameter, aspect ratio AR, and purity) are summarized in Table I.

The MWCNTs were mixed with commercial thermosetting resin (Epilox) produced by Leuna-Harze (Leuna, Germany). This polymer matrix is a bicomponent resin made with a resin and a hardener. The resin (T-19-36/700) is a colorless, low viscosity (650–750 MPa s at 25 °C) epoxy resin with reduced crystallization tendency and a density of 1.14 g cm⁻³. The chemical composition of Epilox resin T19-36/700 is mainly bisphenol A (30–60 wt%), with the addition of crystalline silica (quartz) (1–10 wt%), glycidyl ether (1–10 wt%), and inner fillers (10–60 wt%). The hardener (H10-31) is a liquid, colorless, low viscosity (400–600 MPa s at 25 °C) modified cycloaliphatic polyamine epoxy adduct with a density 1 g cm⁻³. The resin/hardener ratio used in this work is 100/56 as suggested by Leuna-Harze.

B. NC production

NCs with different MWCNT wt% based on epoxy resin were prepared using the following procedure: 100 parts of resin were first mixed at room temperature with an appropriate amount of preweighed MWCNTs, using an ULTRA-TURRAX[®] mixer (IKA[®]-Werke

TABLE I. Geometrical characteristics and purity of the MWCNTs considered in this work.

| Acronym | Diameter <i>D</i> (nm) | Length <i>L</i> (μm) | Aspect ratio [<i>L/D</i>] | Purity (%) |
|---------|---------------------------|-------------------------|--------------------------------|---------------|
| E15 | 25–45 | >10 | >280 | ≤98.5 |
| E16 | 6–10 | >10 | >1250 | ≤94 |

TABLE II. Raman characteristics of MWCNTs (for symbols description see the text).

| MWCNTs | <i>I_D/I_G</i> | <i>I_D'/I_G'</i> |
|--------|------------------------------------|--------------------------------------|
| E15 | 0.61 | 0.76 |
| E16 | 0.91 | 1.38 |

GmbH & Co. KG, Staufen, Germany). This mixer works in the range from 3000 to 25,000 rpm and it was selected to achieve a homogeneous dispersion of carbon filler inside the resin. A homogeneous dispersion of the nanofiller is crucial to obtain a uniform performance of the final product.⁷ Inhomogeneity and aggregates of filler lead, in fact, to a nonuniformity in the characteristics of the NCs. Finally, the hardener was added. The composites were mechanically mixed for several minutes and after that the liquid was poured into a cylindrical mold, taking particular care to avoid the incorporation of air. Air bubbles as well as the aggregates of the nanofiller could lead to a nonuniform final product. Moreover, air bubbles incorporated are random in size and distribution, damaging the reproducibility of the properties. Therefore, the mold filled with the composite was placed in a vacuum chamber to remove the possible air bubbles present inside the sample. Finally, the samples were cured in an oven at 74 °C for 4 h, as prescribed in the resin procedure. After overnight recovery at room temperature, samples were removed from the mold.

Dynamic light scattering (DLS) and laser Doppler velocimetry, for the characterization of the size and zeta potential of the composite in the solution, were performed on a Malvern Instruments Zetasizer Nano-ZS instrument. DLS analyzes the velocity distribution of particle movement by measuring the dynamic fluctuations of light scattering intensity caused by the Brownian motion of the particle, and the data are interpreted in terms of zeta potential. Samples for this study were prepared as previously discussed and then diluted 100 times in deionized water, then vortexed to provide a homogeneous solution. The solutions were made at a concentration of CNTs (E15 and E16) of 3 wt% and Epilox.

C. Resistance measurements

A “two point probe (TPP) method”^{16,17} was used to measure the resistivity of the NCs. This method is based on two electrical contacts positioned directly on the sample surface and able to create a stable contact as shown in Fig. 1. The samples were placed on an insulating board to avoid unwanted contributions to the electrical signal. The low conductivity of the samples made the use of the “inline four point probes (FPP) technique”¹⁸ unnecessary. A Keithley-238 high current source measure unit was used as a high voltage source, coupled with a nanoamperometer. The source can apply voltages in the range ± 110 V and measure currents from ±10 fA up to ± 1 A (at ± 15 V). In fact, the electrical DC current values were recorded for voltages ranging from –10 V to + 10 V with a 0.1 V step. Each sample was measured several times for different electrode placements, to have a meaningful statistical average value for the resistance values and to test the sample uniformity.

D. Low-frequency permittivity measurements

The permittivity of thin samples can be measured using a parallel plate capacitor, as the relation between capacitance and plate separation is very simple for an ideal

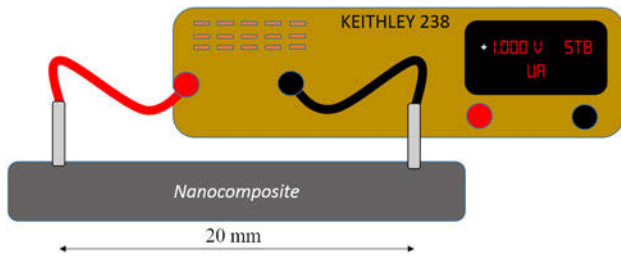


FIG. 1. TPP set up.

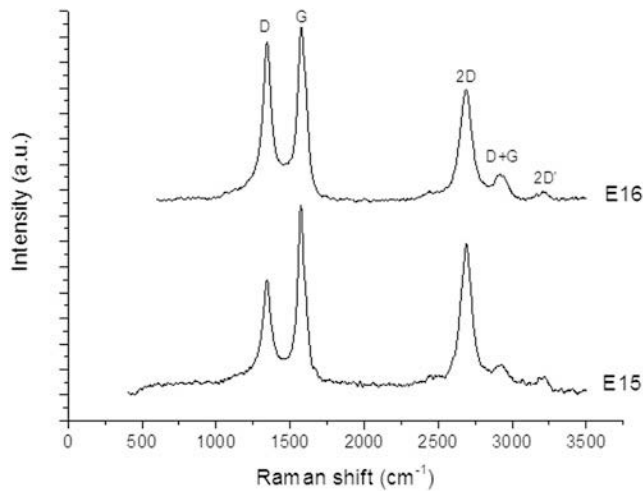


FIG. 2. Raman spectra of E15 and E16 MWCNTs and their respective intensity ratio of D and G peaks.

parallel plate capacitor.^{19,20} The impedance values were measured with an HP Impedanzimeter 4192A in the frequency range 100 KHz–12 MHz using a circular disk capacitor. Then, as the complex impedance is defined as $Z = G + j\omega C$, the real and imaginary parts of the permittivity were obtained as:

$$\epsilon' = \frac{C}{S} \quad \epsilon'' = \frac{G}{\omega S} \quad (1)$$

where C is the capacitance (F), G is the conductance, S is the shape factor that depends on the area of the plate and on the thickness of the sample, and $\omega = 2\pi f$ is the angular frequency.

III. RESULTS AND DISCUSSION

A. Material characterization

The characteristics of MWCNTs were investigated using Raman analysis (see Fig. 2). The intensity ratio of the D peak (centered at about 1360 cm^{-1} and correlated with carbon structure disorder) and the G peak (centered around 1580 cm^{-1} and related to the graphitization grade) is lower for E15 than for E16. For further information, we report in Table II the I_D/I_G and I_{2D}/I_G ratio.

As shown in Figs. 3(a) and 3(b), the MWCNTs have diameters in the range 25–45 nm for E15 and 6–10 nm for E16. Both types of MWCNTs appear entangled and E15 has a lower defectiveness compared to E16, as confirmed by Raman analysis.

The dispersion of MWCNTs inside the resin is crucial to guarantee the homogeneity of the samples. To analyze the dispersion of the filler in the NCs, their internal surface was analyzed by means of FESEM

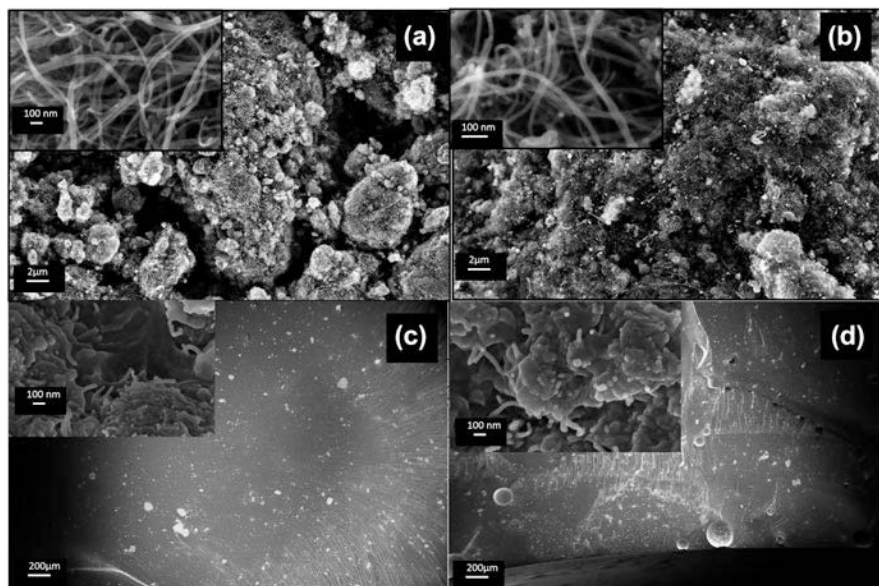


FIG. 3. FESEM for (a) E15, (b) E16 and NCs made by (c) E15, and (d) E16. High-resolution in the inset figure.

(Zeiss 40, Field Emission Scanning Electron Microscopy, Oberkochen, Germany). To obtain an unblemished surface, the cryofracture method was used. This consists of immersing the sample in a liquid nitrogen (77 K, $-196\text{ }^{\circ}\text{C}$) to achieve rapid freezing. After 5 min of immersion, the sample is removed from the liquid nitrogen and immediately broken into pieces by fast mechanical compression. This technique helps to maintain the internal structure of the specimens, avoiding resin elongation with subsequent MWCNT reorientation. The cryofractured samples were coated in a thick chromium layer of a few nanometers ($<10\text{ nm}$), to allow FESEM analysis despite the low electrical conductivity of most samples.

The effects of different ultra-turrax[®] times were analyzed on a 3 wt% concentration by means of zeta potential (ζ -potential,²¹) (see Fig. 4). Note that, for E15, increasing the ultra-turrax[®] time, the zeta potential increases. The solution reaches moderate stability at 5 min ($\zeta < -30$). Nevertheless, a further increase of the ultra-turrax[®] time does not produce any benefit in terms of the stability of the solution (ns). For E16, instead, the solution never reaches stability in terms of dispersion. Figure 4 (left panel) shows a significant variation of the zeta potential, increasing the ultra-turrax[®] time to 3 and 5 min but still unable to

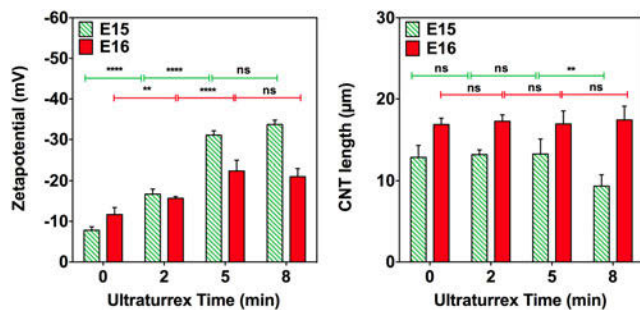


FIG. 4. Effects of increasing ultra turax times on dispersion of E15 and E16 CNTs (left panel). Analysis of CNTs length (right panel).

produce a stable solution ($-30 < \zeta < -10$). Moreover, further increasing the dispersion time to 8 min, the degree of dispersion does not increase significantly compared to the result obtained with 5 min.

The nominal lengths of CNTs was verified by means of TEM images of the diluted solutions, taken for several data points at different ultra-turrax[®] times. The images were processed and analyzed with ImageJ for retrieving information about the length. Only in the case of 8 min of ultra-turrax[®] time for E15, a significative reduction of the length of the CNT can be observed.

The performances of the NCs can also be influenced by others parameters such as, for example, the velocity of mixing and the duration of the drying process in the oven. The velocity of mixing was chosen to avoid the presence of air bubbles entrapped in the polymer matrix as much as possible. Moreover, to avoid air bubbles trapped in the polymer matrix, a vacuum treatment was made on all the samples.

B. Electrical resistivity

The electrical resistivity was measured as described in Sec. II. The I-V characteristics were obtained for the pure epoxy resin and for each NC type I (see Fig. 5). The reproducibility of the measurements is good and each curve reported is obtained by at least three different measurements, changing the probe position on the surface of the NCs. After obtaining the total current I generated by an applied voltage V , the macroscopic electrical conductivity σ of the NCs can be evaluated according to Ohm's law:

$$\sigma = \frac{I l}{V A}, \quad (2)$$

where l is the distance between the two electrodes and A is the cross-sectional area of the electrode. For the contact area $A = 1\text{ mm}^2$ and $l = 20\text{ mm}$, a ratio $l/A = 2 \cdot 10^{-4}\text{ m}^{-1}$ can be obtained. The values of the DC electrical conductivity are reported in Fig. 5. This figure also shows that for

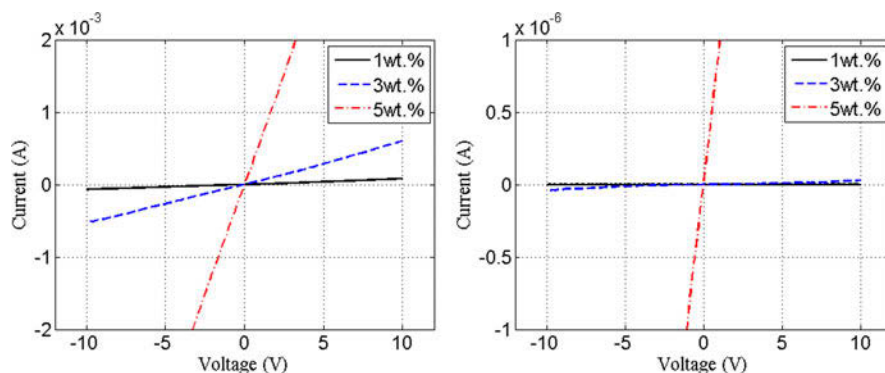


FIG. 5. I-V characteristics for E16 (left panel) and E15 (right panel).

the same wt% concentration, the conductivity of E15 MWCNTs increases more than in the case of E16 MWCNTs. This behavior can be correlated with the difference in diameters between the two types of MWCNT. Thinner CNTs have a lower mass per CNT as the mass of individual CNTs of similar length roughly scales with the square of the diameter. Hence, for the same wt% concentration, the number density is approximately 20 times greater for E16 thus resulting in shorter distances between neighboring CNTs. The reduction of the distances the electrons have to travel inside the highly resistive resin eventually leads to higher electrical conductivities. It should be noted that a role is also played by CNT quality (i.e., impurities amount and nature of

impurities) and the quality of dispersion (agglomeration increases the distances traveled by electrons inside the matrix). As E16 is not so efficiently dispersed and of lower quality, the overall results are consistent.

In Fig. 6, the conductivity values for different values of wt% concentration are shown.

C. Low-frequency permittivity

The measurement set up described in Sec. II was first tested on some reference materials used as substrates in printed circuit boards (dielad, FR4) and on pure Epilox that was used as a matrix for the dispersion of the MWCNTs. The results obtained were consistent with those presented in the literature.^{22,23}

The real parts of the permittivity and the conductivity of E15 and E16 are shown in Figs. 7 and 8, respectively. A general trend in the reduction of permittivity with an increase in frequency can be seen. An increase in the permittivity with a higher weight percentage of the MWCNTs can also be observed in each case. A difference in the value of the permittivity of E16 as compared to that of E15 is due to their respective percolation thresholds: E15 being 0.3 and E16 being 0.1.²³ A further increase in the permittivity of E15 5 wt% is the result of the aforementioned higher weight percentage. Likewise, the conductivity increases with an increase in the frequency and weight percentage of the MWCNTs.

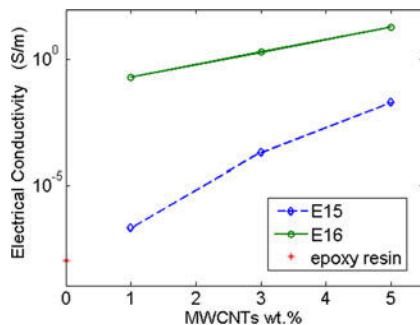


FIG. 6. Conductivity as a function of filler type and wt%.

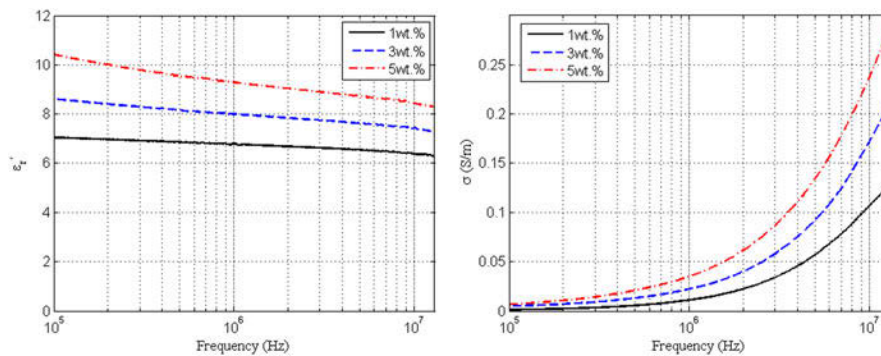


FIG. 7. Relative permittivity (real part) and conductivity of E15 samples.

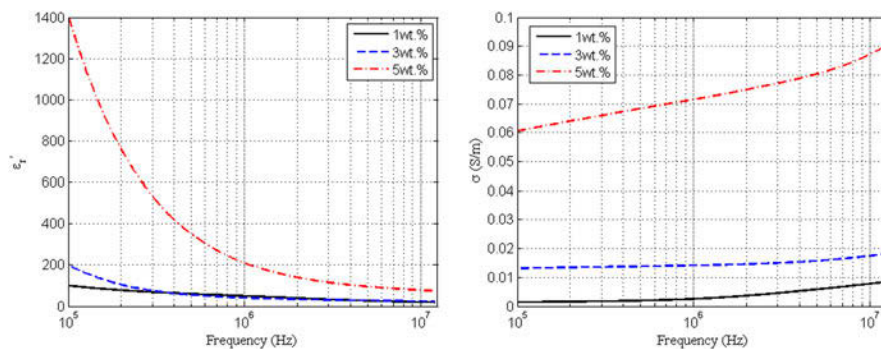


FIG. 8. Relative permittivity (real part) and conductivity of E16 samples.

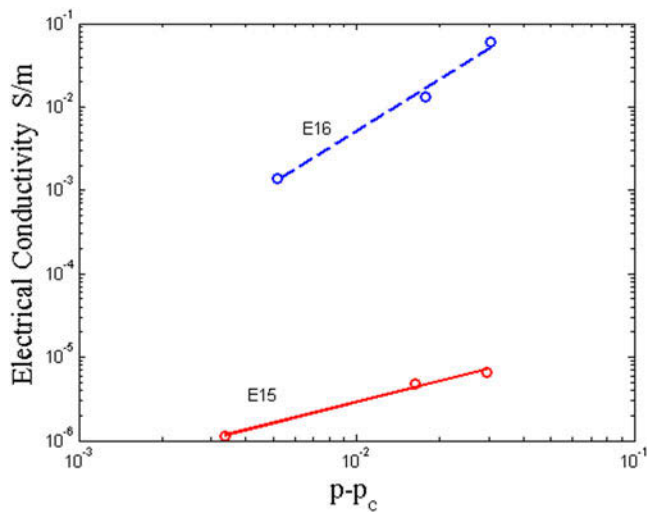


FIG. 9. Log–log plot of the conductivity as a function of $p - p_c$.

According to classical percolation theory, the conductivity of composite materials can be described by the following scaling law:²⁴

$$\sigma \propto (p - p_c)^t, \quad (4)$$

where p is the volume fraction of the filler, p_c is the percolation threshold, and t is a scaling exponent. Figure 9 represents a best fit to the experimentally measured conductivity data as a function of $(p - p_c)$ according to Eq. (4). This analysis reveals a scaling exponent of 0.83 for E15 and of 2.07 for E16. These values are consistent with those reported in the literature.^{25,26}

IV. CONCLUSION

In this paper, the low frequency electrical characterization of NCs made of epoxy resin and MWCNTs has been addressed. Two different types of MWCNTs, one with a low and one with a high aspect ratio, were considered. The dispersion of the filler in the polymer matrix was analyzed by means of a FESEM technique. The I–V characteristics of samples with different concentrations of MWCNTs were obtained. The conductivity values were found to be higher for MWCNTs with thinner diameters (E16). This has been found to be related to the number of MWCNTs present in the NCs at the same wt%. If the number of CNTs increases, as a consequence the distance between the CNTs decreases and a short distance facilitates the conductivity in the NC.

ACKNOWLEDGMENTS

The authors would like to thank Nanothinx for material supplying the materials and Salvatore Guastella for FESEM analysis.

REFERENCES

1. R. Andrews and M.C. Weisenberger: Carbon nanotube polymer composites. *Curr. Opin. Solid State Mater. Sci.* **8**, 31–37 (2004).
2. K. Song, Y. Zhang, J. Meng, E.C. Green, N. Tajaddod, H. Li, and M.L. Minus: Structural polymer-based carbon nanotube composite fibers: Understanding the processing–structure–performance relationship. *Materials* **6**(6), 2543–2577 (2013).
3. X.J. Xu, M.M. Thwe, C. Shearwood, and K. Liao: Mechanical properties and interfacial characteristics of carbon nanotube reinforced epoxy thin film. *Appl. Phys. Lett.* **81**(15), 2833–2835 (2002).
4. F.T. Fisher, R.D. Bradshaw, and L.C. Brinson: Effects of nanotube waviness on the modulus of nanotube-reinforced polymers. *Appl. Phys. Lett.* **80**(24), 4647–4649 (2002).
5. S. Sathyanarayana and C. Hubner: Thermoplastic nanocomposites with carbon nanotubes. *Struct. Nanocompos.* **8**, 19–60 (2013).
6. J.N. Coleman, U. Khan, W.J. Blau, and Y.K. Gun'ko: Small but strong: A review of the mechanical properties of carbon nanotube–polymer composites. *Carbon* **44**, 1624–1652 (2006).
7. R. Coons: Carbon nanotubes' potential spurs investment, scrutiny (review). *Chem. Week* **171**(21), 10 (2009).
8. W. Bauhofer and J.Z. Kovacs: A review and analysis of electrical percolation in carbon nanotube polymer composites. *Compos. Sci. Technol.* **69**(10), 1486–1498 (2009).
9. B.P. Grady: Effects of carbon nanotubes on polymer physics (review). *J. Polym. Sci., Part B: Polym. Phys.* **50**(9), 591 (2012).
10. J.Z. Kovacs, B.S. Velagala, K. Schulte, and W. Bauhofer: Two percolation thresholds in carbon nanotube epoxy composites. *Compos. Sci. Technol.* **67**, 922 (2007).
11. J.K.W. Sandler, J.E. Kirk, I.A. Kinloch, M.S.P. Shaffer, and A.H. Windle: Effects of carbon nanotubes on polymer physics (review): Ultra-low electrical percolation threshold in carbon-nanotube-epoxy, composites. *Polymer* **44**, 5893–5899 (2003).
12. A.N. Lagarkov and A.K. Sarychev: Electromagnetic properties of composites containing elongated conducting inclusions. *Phys. Rev. B* **53**, 6318–6336 (1996).
13. C. Grimaldi, M. Mioni, R. Gaal, F. László, and A. Magrez: Electrical conductivity of multi-walled carbon nanotubes-SU8 epoxy composites. *Appl. Phys. Lett.* **102**, 223114 (2013).
14. B.E. Kilbride, J.N. Coleman, J. Fraysse, P. Fournet, M. Cadek, A. Drury, S. Hutzler, S. Roth, and W.J. Blau: Experimental observation of scaling laws for alternating current and direct current conductivity in polymer-carbon nanotube composite thin films. *J. Appl. Phys.* **9**(7), 4024–4030 (2002).
15. N. Hu, Z. Masuda, C. Yan, G. Yamamoto, H. Fukunaga, and T. Hashida: The electrical properties of polymer nanocomposites with carbon nanotube fillers. *Nanotechnology* **19**, 215701 (2008).
16. D.K. Schroder: *Semiconductor Material, and Device Characterization* (Wiley Inter-Science Publications, 1990).
17. A.S. Grove: *Physics and Technology of Semiconductor Device* (Wiley & Sons, New York, NY, 1993).
18. A. Chiolerio, M. Castellino, P. Jagdale, M. Giorcelli, S. Bianco, and A. Tagliaferro: Electrical properties of CNT-based polymeric matrix nanocomposites In: *Carbon Nanotubes - Polymer Nanocomposites*, Siva Yellampalli ed.; INTECH Open Access Publisher, Rijeka, Croatia, 2011; pp. 215–230.
19. H. Nishiyama and M. Nakamura: Capacitance of disk capacitors. *IEEE Trans. Compon., Hybrids, Manuf. Technol.* **16**(3), 360 (1993).
20. T.T. Grove, M.F. Masters, and R.E. Miers: Determining dielectric constant using a parallel plate capacitor. *American Association of Physics Teachers* **73**(1), 52 (2005).
21. S. Levine, J.R. Marriott, G. Neale, and N. Epstein: Theory of electrokinetic flow in fine cylindrical capillaries at high zeta-potentials. *J. Colloid Interface Sci.* **52**(1), 136–149 (July 1975).

22. A.J. Djordjevic, R.M. Biljic, V.D. Likar-Smiljanic, and T.K. Sarkar: Wideband frequency-domain characterization of FR-4 and time-domain causality. *IEEE Trans. Electromagn. Compat.* **43**(4), 662 (2001).
23. P. Savi, M. Miscuglio, M. Giorcelli, and A. Tagliaferro: Analysis of microwave absorbing properties of epoxy MWCNT composites. *Prog. Electromagn. Res. Lett.* **44**, 63–66 (2014).
24. D. Stauffer and A. Aharony: *Introduction to Percolation Theory* (Taylor and Francis, London, 1994).
25. B.E. Kilbride, J.N. Coleman, J. Fraysse, P. Fournet, M. Cadek, A. Drury, S. Hutzler, S. Roth, and W.J. Blau: Experimental observation of scaling laws for alternating current and direct current conductivity in polymer-carbon nanotube composite thin films. *J. Appl. Phys.* **92**(7), 4024–4030 (2002).
26. J. Zhang, M. Mine, D. Zhu, and M. Matsuo: Electrical and dielectric behaviors and their origins in the three-dimensional polyvinyl alcohol/MWCNT composites with low percolation threshold. *Carbon* **47**(5), 1311–1320 (2009).